Original Article
International Journal of Fuzzy Logic and Intelligent Systems
Vol. 13, No. 3, September 2013, pp. 154-163
http://dx.doi.org/10.5391/IJFIS.2013.13.3.154

ISSN(Print) 1598-2645
ISSN(Online) 2093-744X

Formation Control for Underactuated Autonomous Underwater Vehicles Using the Approach Angle

Kyoung Joo Kim[1], Jin Bae Park[1], and Yoon Ho Choi[2]
[1]Department of Electrical and Electronic Engineering, Yonsei University, Seoul, Korea
[2]Department of Electronic Engineering, Kyonggi University, Suwon, Korea

ljfis

Abstract

In this paper, we propose a formation control algorithm for underactuated autonomous underwater vehicles (AUVs) with parametric uncertainties using the approach angle. The approach angle is used to solve the underactuated problem for AUVs, and the leader-follower strategy is used for the formation control. The proposed controller considers the nonzero off-diagonal terms of the mass matrix of the AUV model and the associated parametric uncertainties. Using the state transformation, the mass matrix, which has nonzero off-diagonal terms, is transformed into a diagonal matrix to simplify designing the control. To deal with the parametric uncertainties of the AUV model, a self-recurrent wavelet neural network is used. The proposed formation controller is designed based on the dynamic surface control technique. Some simulation results are presented to demonstrate the performance of the proposed control method.

Keywords: Formation control, Leader-follower strategy, Autonomous underwater vehicle, Underactuated systems, Dynamic surface control

1. Introduction

Over the last two decades, the research and development of autonomous underwater vehicles (AUVs) and surface vessels have been important issues because of their usefulness in performing missions such as environmental surveying, undersea cable/pipeline inspection, monitoring of coastal shallow-water regions, and offshore oil installations [1-5].

In addition, since performing offshore missions is more efficiently accomplished by using multiple AUVs rather than a single AUV, a large number of studies have been published concerning the formation control of multiple AUVs. There are three popular strategies in designing the formation controller: the behavior-based strategy [6], the virtual structure strategy [7-8], and the leader-follower strategy [9-11]. Among these methods, the leader-follower method is most widely used by many researchers due to advantages such as simplicity and scalability. In the leader-follower method, the leader tracks a predefined trajectory and the follower maintains a desired separation-bearing/separation-separation configuration with the leader. The follower can be designated as a leader for other vehicles because of the scalability of formation. In addition, the leader-follower method is simple to implement since the reference trajectory of the follower is clearly defined by the leader's movement, and the internal formation stability is induced by the control laws of the individual vehicles. A leader-

Received: Jul. 26, 2013
Revised : Sep. 13, 2013
Accepted: Sep. 14, 2013

Correspondence to: Jin Bae Park
(jbpark@yonsei.ac.kr)

follower formation controller for underactuated AUVs was proposed in [11], in which the controller needs an "exogenous" system and this exogenous system must know each vehicle position. Skejetne proposed a formation controller such that each individual vehicle has a position relative to a point called the formation reference point [12]. However, these papers did not consider the off-diagonal terms in the system matrix or the parametric uncertainties of the AUV.

In this paper, therefore, we propose a formation control algorithm for underactuated AUVs. First, we obtain the virtual leader in reference to the follower in the leader-follower strategy; the formation problem is then dealt with as a tracking problem. Second, in order to design the controller, we use the state transformation [13], which can avoid the difficulties caused by the off-diagonal terms in the system matrix, and we employ self-recurrent wavelet neural networks (SRWNNs) [14, 15] to deal with the uncertainties in the hydrodynamic damping terms. Third, using the approach angle [16] and the formation error dynamics in the body-fixed frame, we solve the underactuated problem for AUVs. Fourth, the dynamic surface control (DSC) technique [17], which can solve the "explosion of complexity" problem caused by the repeated differentiation of virtual controllers in the backstepping design procedure, is applied to design the formation controller for underactuated AUVs. Finally, we perform computer simulations to illustrate the performance of the proposed controller.

2. Preliminaries

2.1 Asymmetric Structured AUV Dynamics

The asymmetric structured AUV has nonzero off-diagonal terms in the mass matrix, which are induced by the asymmetric shape of the bow and the stern of the vehicle. The kinematics and dynamics of the asymmetric AUV are described as follows [13]:

$$\dot{\mathrm{v}}= \mathrm{J}\left(\psi\right)\eta$$

$$\mathrm{M}\dot{\nu}= -\mathrm{C}\left(\nu\right)\nu-\mathrm{D}\left(\nu\right)\nu+\tau, \tag{1}$$

where $\eta= \left[\mathrm{x}\ \ \mathrm{y}\ \ \psi\right]^{\mathrm{T}}$ denotes the position (x, y) and the yaw angle ψ of the AUV in the earth-fixed frame, $\nu= \left[\mathrm{u}\ \ \mathrm{v}\ \ \mathrm{r}\right]^{\mathrm{T}}$ is a vector denoting the surge, sway, and yaw velocities of the AUV in the body-fixed frame, respectively, and $\tau= \left[\tau_{\mathrm{u}}\ \ 0\ \ \tau_{\mathrm{r}}\right]^{\mathrm{T}}$ is the control vector of the surge force τ_{u} and yaw moment τ_{r}. In the above equation, the matrices $\mathrm{J}\left(\psi\right)$, $\mathrm{D}\left(\nu\right)$, $\mathrm{C}(\nu)$, and M are given as follows:

$$\mathrm{J}\left(\psi\right)= \begin{bmatrix} \cos\psi & -\sin\psi & 0 \\ \sin\psi & \cos\psi & 0 \\ 0 & 0 & 1 \end{bmatrix},$$

$$\mathrm{D}\left(\eta\right)= -\begin{bmatrix} \mathrm{d}_{11}(\mathrm{u}) & 0 & 0 \\ 0 & \mathrm{d}_{22}(\mathrm{v},\mathrm{r}) & \mathrm{d}_{23}(\mathrm{v},\mathrm{r}) \\ 0 & \mathrm{d}_{32}(\mathrm{v},\mathrm{r}) & \mathrm{d}_{33}(\mathrm{v},\mathrm{r}) \end{bmatrix},$$

$$\mathrm{C}\left(\eta\right)= \begin{bmatrix} 0 & 0 & -\mathrm{m}_{22}\mathrm{v}-\mathrm{m}_{23}\mathrm{r} \\ 0 & 0 & \mathrm{m}_{11}\mathrm{u} \\ \mathrm{m}_{22}\mathrm{v}+\mathrm{m}_{23}\mathrm{r} & -\mathrm{m}_{11}\mathrm{u} & 0 \end{bmatrix},$$

$$\mathrm{M}= \begin{bmatrix} \mathrm{m}_{11} & 0 & 0 \\ 0 & \mathrm{m}_{22} & \mathrm{m}_{23} \\ 0 & \mathrm{m}_{32} & \mathrm{m}_{33} \end{bmatrix},$$

where

$$\begin{aligned} \mathrm{m}_{11} &= \mathrm{m}-\mathrm{X}_{\dot{\mathrm{u}}}, \mathrm{m}_{22}= \mathrm{m}-\mathrm{Y}_{\dot{\mathrm{v}}}, \mathrm{m}_{23}= \mathrm{m}\mathrm{x}_{\mathrm{g}}-\mathrm{Y}_{\dot{\mathrm{r}}}, \\ \mathrm{m}_{33} &= \mathrm{I}_{\mathrm{z}}-\mathrm{N}_{\dot{\mathrm{r}}}, \mathrm{d}_{11}\left(\mathrm{u}\right)= -(\mathrm{X}_{\mathrm{u}}+\mathrm{X}_{\mathrm{u}|\mathrm{u}|}\left|\mathrm{u}\right|), \\ \mathrm{d}_{22}\left(\mathrm{v},\mathrm{r}\right) &= -(\mathrm{Y}_{\mathrm{v}}+\mathrm{Y}_{\mathrm{v}|\mathrm{v}|}+\mathrm{Y}_{\mathrm{r}|\mathrm{v}|}\left|\mathrm{r}\right|), \\ \mathrm{d}_{23}\left(\mathrm{v},\mathrm{r}\right) &= -(\mathrm{Y}_{\mathrm{r}}+\mathrm{Y}_{\mathrm{v}|\mathrm{r}|}+\mathrm{Y}_{\mathrm{r}|\mathrm{r}|}\left|\mathrm{r}\right|), \\ \mathrm{d}_{32}\left(\mathrm{v},\mathrm{r}\right) &= -(\mathrm{N}_{\mathrm{v}}+\mathrm{N}_{\mathrm{v}|\mathrm{v}|}\left|\mathrm{v}\right|+\mathrm{N}_{\mathrm{r}|\mathrm{v}|}\left|\mathrm{r}\right|), \\ \mathrm{d}_{33}\left(\mathrm{v},\mathrm{r}\right) &= -(\mathrm{N}_{\mathrm{r}}+\mathrm{N}_{\mathrm{v}|\mathrm{r}|}\left|\mathrm{v}\right|+\mathrm{N}_{\mathrm{r}|\mathrm{r}|}\left|\mathrm{r}\right|). \end{aligned}$$

Here, X_{u}, $\mathrm{X}_{\mathrm{u}|\mathrm{u}|}$, Y_{v}, $\mathrm{Y}_{|\mathrm{v}|\mathrm{v}}$, $\mathrm{Y}_{|\mathrm{r}|\mathrm{v}}$, Y_{r}, $\mathrm{Y}_{|\mathrm{v}|\mathrm{r}}$, $\mathrm{Y}_{\mathrm{r}|\mathrm{r}|}$, N_{v}, $\mathrm{N}_{|\mathrm{v}|\mathrm{v}}$, $\mathrm{N}_{|\mathrm{r}|\mathrm{v}}$, N_{r}, $\mathrm{N}_{|\mathrm{v}|\mathrm{r}}$, and $\mathrm{N}_{|\mathrm{r}|\mathrm{r}}$ are the linear and quadratic drag coefficients; m is the mass of the AUV; $\mathrm{X}_{\dot{\mathrm{u}}}$, $\mathrm{Y}_{\dot{\mathrm{v}}}$, $\mathrm{Y}_{\dot{\mathrm{r}}}$, and $\mathrm{N}_{\dot{\mathrm{r}}}$ are the added masses; x_{g} is the x-coordinate of the center of gravity (COG) of the AUV in the body-fixed frame; and I_{z} is the inertia with respect to the vertical axis.

Here the matrix M includes the off-diagonal term m_{23}, which is present because the shape of bow is in general different from that of stern. Therefore, the sway dynamics is are affected by the yaw moment τ_{r} because of the parameter m_{23}. Furthermore, there are only two control inputs: the surge force τ_{u} and yaw moment τ_{r}. The number of control inputs is less than the number of degrees of freedom of the AUV in the horizontal plane. Moreover, the parameters of the AUV model (1) cannot be obtained exactly. Therefore, it is difficult to design the controller for the underactuated AUV, which has both off-diagonal terms and model uncertainties.

2.2 State Transformation

Since the yaw moment τ_{r} acts directly on the sway dynamics in (1), causing difficulty in designing the controller, we use the

following state transformations [13]:

$$\begin{aligned}\overline{\mathrm{x}} &= \mathrm{x} + \epsilon\cos\psi,\\ \overline{\mathrm{y}} &= \mathrm{y} + \epsilon\sin\psi,\\ \overline{\mathrm{v}} &= \mathrm{v} + \epsilon\mathrm{r},\end{aligned} \tag{2}$$

where $\epsilon = \mathrm{m}_{23}/\mathrm{m}_{22}$. The transformed equation (2) indicates that the virtual center of mass is positioned by ϵ in the longitudinal direction. Using (2), the AUV dynamics (1) can be rewritten as

$$\begin{aligned}\dot{\overline{\mathrm{x}}} &= \mathrm{u}\cos\psi - \overline{\mathrm{v}}\sin\psi\ ,\\ \dot{\overline{\mathrm{y}}} &= \mathrm{u}\sin\psi - \overline{\mathrm{v}}\cos\psi\ ,\\ \dot{\psi} &= \mathrm{r},\\ \dot{\mathrm{u}} &= \varphi_{\mathrm{u}} + \frac{1}{\mathrm{m}_{11}}\tau_{\mathrm{u}},\\ \dot{\overline{\mathrm{v}}} &= \varphi_{\mathrm{v}} + \frac{\mathrm{m}_{23}}{\mathrm{m}_{22}}\varphi_{\mathrm{r}},\\ \dot{\mathrm{r}} &= \varphi_{\mathrm{r}} + \frac{\mathrm{m}_{22}}{\mathrm{m}_{22}\mathrm{m}_{33} - \mathrm{m}^2{}_{23}}\tau_{\mathrm{r}},\end{aligned} \tag{3}$$

where

$$\begin{aligned}\varphi_{\mathrm{u}} &= \frac{\mathrm{m}_{22}}{\mathrm{m}_{11}}\mathrm{vr} + \frac{\mathrm{m}_{23}}{\mathrm{m}_{11}}\mathrm{r}^2 - \frac{\mathrm{d}_{11}(\mathrm{u})}{\mathrm{m}_{11}}\mathrm{u},\\ \varphi_{\mathrm{v}} &= -\frac{\mathrm{m}_{11}}{\mathrm{m}_{22}}\mathrm{ur} - \frac{\mathrm{d}_{22}(\mathrm{v},\mathrm{r})}{\mathrm{m}_{22}}\mathrm{v} - \frac{\mathrm{d}_{23}(\mathrm{v},\mathrm{r})}{\mathrm{m}_{22}}\mathrm{r},\\ \varphi_{\mathrm{r}} &= \frac{1}{\mathrm{m}_{22}\mathrm{m}_{33} - \mathrm{m}^2{}_{23}}\{\left(\mathrm{m}_{11}\mathrm{m}_{22} - \mathrm{m}^2{}_{22}\right)\mathrm{uv}\\ &\quad + \left(\mathrm{m}_{11}\mathrm{m}_{23} - \mathrm{m}_{23}\mathrm{m}_{22}\right)\mathrm{ur}\\ &\quad - \left(\mathrm{d}_{33}(\mathrm{v},\mathrm{r})\,\mathrm{r} + \mathrm{d}_{32}(\mathrm{v},\mathrm{r})\,\mathrm{v}\right)\mathrm{m}_{22}\\ &\quad + \left(\mathrm{d}_{23}(\mathrm{v},\mathrm{r})\,\mathrm{r} + \mathrm{d}_{22}(\mathrm{v},\mathrm{r})\,\mathrm{v}\right)\mathrm{m}_{23}\}.\end{aligned} \tag{4}$$

Remark 1. Here, we assume that we do not know the exact values of φ_{u}, φ_{v}, and φ_{r} since the parameters of the system matrices cannot be obtained exactly by measurement or by calculation. Since the system matrices inevitably have uncertainties, we employ a SRWNN to compensate for the parametric uncertainties of φ_{u}, φ_{v}, and φ_{r}. The estimated parameters $\widehat{\varphi}_{\mathrm{u}}$, $\widehat{\varphi}_{\mathrm{v}}$, and $\widehat{\varphi}_{\mathrm{r}}$ of φ_{u}, φ_{v}, and φ_{r} comprise the SRWNN.

2.3 Self-Recurrent Wavelet Neural Network

In this paper, we use a SRWNN to compensate for the parametric uncertainties of the AUV model. The SRWNN structure, which has $\mathrm{N_i}$ inputs, one output, and $\mathrm{N_i} \times \mathrm{N_w}$ mother wavelets, consists of four layers: an input layer, a mother wavelet layer, a product layer, and an output layer. The SRWNN output is composed of self-recurrent wavelets and parameters such that

$$\mathrm{y} = \sum_{\mathrm{n}=1}^{\mathrm{N_w}} \omega_{\mathrm{n}} \left(\prod_{\mathrm{k}=1}^{\mathrm{N_i}} \Phi_{\mathrm{nk}}\left(\mathrm{g_{nk}}(\mathrm{N})\right) \right) + \sum_{\mathrm{k}=1}^{\mathrm{N_i}} \mathrm{a_k}\chi_{\mathrm{k}}(\mathrm{N}), \tag{5}$$

where the subscript *n*k indicates the *k*-th input term of the *n*-th wavelet, N denotes the number of iterations, the output y is the estimate of the uncertainty, χ_{k} denotes the *k*-th input of the SRWNN, $\mathrm{a_k}$ is the connection weight between the input nodes and the output node, ω_{n} is the connection weight between the product nodes and the output nodes, and $\mathrm{g_{nk}}(\mathrm{N}) = (\chi_{\mathrm{k}}(\mathrm{N}) + \Phi_{\mathrm{nk}}(\mathrm{N}-1) \times \vartheta_{\mathrm{nk}} - \varrho_{\mathrm{nk}})/\mu_{\mathrm{nk}}$. Here, ϱ_{nk}, μ_{nk}, and ϑ_{nk} are the translation factor, dilation factor, and weight of the self-feedback loop, respectively. The memory term $\Phi_{\mathrm{nk}}(\mathrm{N}-1)$ denotes the one step recurrent term of a wavelet. In addition, the mother wavelets are chosen as the first derivatives of a Gaussian function $\Phi_{\mathrm{nk}}(\mathrm{g_{nk}}) = -\mathrm{g_{nk}}\mathrm{e}^{-\frac{1}{2}\mathrm{g_{nk}}^2}$, which has the universal approximation property [18]. In this paper, the five weights $\mathrm{a_k}$, ϱ_{nk}, μ_{nk}, ϑ_{nk}, and ω_{n} of the SRWNN will be trained online by the adaptation laws based on the Lyapunov theory.

The weighting vector $\mathrm{W} \in \mathbb{R}^{3\mathrm{N_i}\mathrm{N_w}+\mathrm{N_i}+\mathrm{N_w}}$ is defined as follows:

$$\begin{aligned}\mathrm{W} = [&(\mathrm{a_k})_{(1\le\mathrm{k}\le\mathrm{N_i})} \quad (\varrho_{\mathrm{nk}})_{(1\le\le\mathrm{N_i},\ 1\le\mathrm{n}\le\mathrm{N_w})}\\ &(\mu_{\mathrm{nk}})_{(1\le\mathrm{k}\le\mathrm{N_i},/1\le\mathrm{n}\le\mathrm{N_w})} \quad (\vartheta_{\mathrm{nk}})_{(1\le\mathrm{k}\le\mathrm{N},\ 1\le\mathrm{n}\le\mathrm{N_w})}\\ &(\omega_{\mathrm{n}})_{(1\le\mathrm{n}\le\mathrm{N_w})}]^T.\end{aligned} \tag{6}$$

According to the powerful approximation ability [18], the SRWNN $\widehat{\varphi}_{\mathrm{j}}$ can approximate the uncertainty term φ_{j} to a sufficient degree of accuracy as follows:

$$\begin{aligned}\varphi_{\mathrm{j}}(\chi_{\mathrm{j}}) &= \widehat{\varphi}_{\mathrm{j}}\left(\chi_{\mathrm{j}} \mid \mathrm{W_j^*}\right) + \delta_{\mathrm{j}}(\chi_{\mathrm{j}})\\ &= \widehat{\varphi}_{\mathrm{j}}\left(\chi_{\mathrm{j}} \mid \widehat{\mathrm{W}}_{\mathrm{j}}\right) + [\widehat{\varphi}_{\mathrm{j}}\left(\chi_{\mathrm{j}} \mid \mathrm{W_j^*}\right) - \widehat{\varphi}_{\mathrm{j}}\left(\chi_{\mathrm{j}} \mid \widehat{\mathrm{W}}_{\mathrm{j}}\right)]\\ &\quad + \delta_{\mathrm{j}}(\chi_{\mathrm{j}}),\end{aligned} \tag{7}$$

where j = u, v, r and $\chi_{\mathrm{j}} \in \kappa_{\chi\mathrm{j}} \subset \mathbb{R}^{10}$ is the input vector of the SRWNN, $\mathrm{W_j^*}$ and $\widehat{\mathrm{W}}_{\mathrm{j}} = \mathrm{diag}(\mathrm{W_j})$, are the optimal and estimated matrices of the weighting vector of the SRWNN defined in (6), respectively, and $\delta_{\mathrm{j}}(\overline{\mathcal{X}}_{\mathrm{j}})$ is the bounded reconstruction error. The optimal parameter vector $\mathrm{W_j^*}$ is given as

$$\mathrm{W_j^*} = \arg\min_{\widehat{\mathrm{W}}_{\mathrm{j}} \in \mathbb{R}^{\alpha}} \left[\sup_{\chi_{\mathrm{j}} \in \kappa_{\chi\mathrm{j}}} \| \varphi_{\mathrm{j}}(\chi_{\mathrm{j}}) - \widehat{\varphi}_{\mathrm{j}}\left(\chi_{\mathrm{j}} \mid \widehat{\mathrm{W}}_{\mathrm{j}}\right) \| \right],$$

where $\alpha = 3\mathrm{N_i}\mathrm{N_w} + \mathrm{N_i} + \mathrm{N_w}$.

Assumption 1. The optimal weight matrix is bounded such that $\left\|\mathrm{W_j^*}\right\|_{\mathrm{F}} \le \mathrm{W_{Mj}}$, where $\|\cdot\|_{\mathrm{F}}$ denotes the Frobenius norm.

Taking the Taylor expansion of $\widehat{\varphi}_{\mathrm{j}}\left(\chi_{\mathrm{j}} \mid \mathrm{W}_{\mathrm{j}}^{*}\right)$ around $\widehat{\mathrm{W}}_{\mathrm{j}}$, we can obtain [19].

$$\widehat{\varphi}_{\mathrm{j}}\left(\chi_{\mathrm{j}} \mid \mathrm{W}_{\mathrm{j}}^{*}\right)-\widehat{\varphi}_{\mathrm{j}}\left(\chi_{\mathrm{j}} \mid \widehat{\mathrm{W}}_{\mathrm{j}}\right)=\widetilde{\mathrm{W}}_{\mathrm{j}}^{\mathrm{T}} \Theta_{\mathrm{j}}+\mathrm{G}_{\mathrm{j}} \mid\left(\widetilde{\mathrm{W}}_{\mathrm{j}}\right), \quad (8)$$

where $\Theta_{\mathrm{j}}=\left[\frac{\partial \widehat{\varphi}_{\mathrm{j},1}}{\partial \widehat{\mathrm{W}}_{\mathrm{j},1}}, \frac{\partial \widehat{\varphi}_{\mathrm{j},2}}{\partial \widehat{\mathrm{W}}_{\mathrm{j},2}}\right]^{\mathrm{T}}$, $\mathrm{G}_{\mathrm{j}} \mid\left(\widetilde{\mathrm{W}}_{\mathrm{j}}\right)$ denotes the high-order terms, and $\widetilde{\mathrm{W}}_{\mathrm{j}}=\mathrm{W}_{\mathrm{j}}^{*}-\widehat{\mathrm{W}}_{\mathrm{j}}$ is the estimation error. Substituting (8) into (7), we have [20]

$$\varphi_{\mathrm{j}}\left(\chi_{\mathrm{j}}\right)=\widehat{\varphi}_{\mathrm{j}}\left(\chi_{\mathrm{j}} \mid \widehat{\mathrm{W}}_{\mathrm{j}}\right)+\widetilde{\mathrm{W}}_{\mathrm{j}}^{\mathrm{T}} \Theta_{\mathrm{j}}+\xi_{\mathrm{j}}, \quad (9)$$

$$\left\|\xi_{\mathrm{j}}\right\| \leq \epsilon_{1 \mathrm{j}}, \quad (10)$$

where $\xi_{\mathrm{j}}=\mathrm{G}_{\mathrm{j}} \mid\left(\widetilde{\mathrm{W}}_{\mathrm{j}}\right)+\delta_{\mathrm{j}}\left(\chi_{\mathrm{j}}\right)$, and $\epsilon_{1 \mathrm{j}}>0$.

3. Main Results

3.1 Controller Design

By the state transformation described in subsection 2.2, the new follower's kinematics and dynamics are as follows:

$$\begin{aligned}
&\overline{\mathrm{x}}_{\mathrm{f}}=\mathrm{x}_{\mathrm{f}}+\epsilon \cos \psi_{\mathrm{f}} \\
&\overline{\mathrm{y}}_{\mathrm{f}}=\mathrm{y}_{\mathrm{f}}+\epsilon \sin \psi_{\mathrm{f}} \\
&\overline{\mathrm{v}}_{\mathrm{f}}=\mathrm{v}_{\mathrm{f}}+\epsilon \mathrm{r}_{\mathrm{f}}.
\end{aligned} \quad (11)$$

Using (11), the follower's dynamics (11) can be rewritten as

$$\begin{aligned}
&\dot{\overline{\mathrm{x}}}_{\mathrm{f}}=\mathrm{u}_{\mathrm{f}} \cos \psi_{\mathrm{f}}-\overline{\mathrm{v}}_{\mathrm{f}} \sin \psi_{\mathrm{f}}, \\
&\dot{\overline{\mathrm{y}}}_{\mathrm{f}}=\mathrm{u}_{\mathrm{f}} \sin \psi_{\mathrm{f}}-\overline{\mathrm{v}}_{\mathrm{f}} \cos \psi_{\mathrm{f}}, \\
&\dot{\psi}_{\mathrm{f}}=\mathrm{r}_{\mathrm{f}}, \\
&\dot{\mathrm{u}}_{\mathrm{f}}=\varphi_{1}+\frac{1}{\mathrm{m}_{11}} \tau_{\mathrm{u}}, \\
&\dot{\overline{\mathrm{v}}}_{\mathrm{f}}=\varphi_{2}+\frac{\mathrm{m}_{23}}{\mathrm{m}_{22}} \varphi_{3}, \\
&\dot{\mathrm{r}}_{\mathrm{f}}=\varphi_{3}+\frac{\mathrm{m}_{22}}{\mathrm{m}_{22} \mathrm{m}_{33}-\mathrm{m}^{2}{}_{23}} \tau_{\mathrm{r}},
\end{aligned} \quad (12)$$

where

$$\begin{aligned}
\varphi_{1}=&\frac{\mathrm{m}_{22}}{\mathrm{m}_{11}} \mathrm{vr}+\frac{\mathrm{m}_{23}}{\mathrm{m}_{11}} \mathrm{r}^{2}-\frac{\mathrm{d}_{11}(\mathrm{u})}{\mathrm{m}_{11}} \mathrm{u}, \\
\varphi_{2}=&-\frac{\mathrm{m}_{11}}{\mathrm{m}_{22}} \mathrm{ur}-\frac{\mathrm{d}_{22}(\mathrm{v}, \mathrm{r})}{\mathrm{m}_{22}} \mathrm{v}-\frac{\mathrm{d}_{23}(\mathrm{v}, \mathrm{r})}{\mathrm{m}_{22}} \mathrm{r}, \\
\varphi_{3}=&\frac{1}{\mathrm{m}_{22} \mathrm{m}_{33}-\mathrm{m}^{2}{}_{23}}\left\{\left(\mathrm{m}_{11} \mathrm{m}_{22}-\mathrm{m}^{2}{}_{22}\right) \mathrm{uv}\right. \\
&+\left(\mathrm{m}_{11} \mathrm{m}_{23}-\mathrm{m}_{23} \mathrm{m}_{22}\right) \mathrm{ur} \\
&-\left(\mathrm{d}_{33}(\mathrm{v}, \mathrm{r}) \mathrm{r}+\mathrm{d}_{32}(\mathrm{v}, \mathrm{r}) \mathrm{v}\right) \mathrm{m}_{22} \\
&\left.+\left(\mathrm{d}_{23}(\mathrm{v}, \mathrm{r}) \mathrm{r}+\mathrm{d}_{22}(\mathrm{v}, \mathrm{r}) \mathrm{v}\right) \mathrm{m}_{23}\right\}.
\end{aligned} \quad (13)$$

According to Remark 1, the hydrodynamic parameters φ_1, φ_2, and φ_3 are estimated by the SRWNN, respectively, as the estimated parameters $\widehat{\varphi}_1$, $\widehat{\varphi}_2$, and $\widehat{\varphi}_3$. Further, to design the formation controller for underactuated AUVs, we obtain the position of the virtual reference vehicle of the followers as follows:

$$\eta_{\mathrm{r}}=\overline{\eta}_{\mathrm{l}}+\mathrm{R}\left(\psi_{\mathrm{l}}\right) \mathrm{l}, \quad (14)$$

where $\eta_{\mathrm{r}}=\left[\mathrm{x}_{\mathrm{r}}, \mathrm{y}_{\mathrm{r}}, \psi_{\mathrm{r}}\right]^{\mathrm{T}}$ is the reference position and yaw angle of the follower; $\overline{\eta}_{\mathrm{l}}=\left[\overline{\mathrm{x}}_{\mathrm{l}}, \overline{\mathrm{y}}_{\mathrm{l}}, \psi_{\mathrm{l}}\right]^{\mathrm{T}}$ is the transformed position and yaw angle of the leader; $\overline{\mathrm{x}}_{\mathrm{l}}=\mathrm{x}+\epsilon \cos \psi_{\mathrm{l}}$ and $\overline{\mathrm{y}}_{\mathrm{l}}=\mathrm{y}+\epsilon \sin \psi_{\mathrm{l}}$ are the transformed positions of the x- and y-coordinates of the leader in the body-fixed frame; ψ_{l} is the yaw of the leader; $\mathrm{l}=\left[\mathrm{l}_{\mathrm{lf}}^{\mathrm{d}} \cos \varphi_{\mathrm{lf}}^{\mathrm{d}}, \mathrm{l}_{\mathrm{lf}}^{\mathrm{d}} \sin \varphi_{\mathrm{lf}}^{\mathrm{d}}, 0\right]^{\mathrm{T}}$; $\mathrm{l}_{\mathrm{lf}}^{\mathrm{d}}$ is the desired distance between the leader and the followers; and $\varphi_{\mathrm{lf}}^{\mathrm{d}}$ is the desired angle between the x-coordinate of the leader in the body-fixed frame and the vector from the leader to the reference vehicle as shown in Figure 1. Using the form of (1), the dynamics of η_{r} can be described as

$$\begin{aligned}
&\dot{\mathrm{x}}_{\mathrm{r}}=\left(\mathrm{u}_{\mathrm{l}}-\mathrm{d}_{\mathrm{y}} \mathrm{r}_{\mathrm{l}}\right) \cos \psi_{\mathrm{l}}-\left(\overline{\mathrm{v}}_{\mathrm{l}}+\mathrm{d}_{\mathrm{x}} \mathrm{r}_{\mathrm{l}}\right) \sin \psi_{\mathrm{l}}, \\
&\dot{\mathrm{y}}_{\mathrm{r}}=\left(\mathrm{u}_{\mathrm{l}}-\mathrm{d}_{\mathrm{y}} \mathrm{r}_{\mathrm{l}}\right) \sin \psi_{\mathrm{l}}-\left(\overline{\mathrm{v}}_{\mathrm{l}}+\mathrm{d}_{\mathrm{x}} \mathrm{r}_{\mathrm{l}}\right) \cos \psi_{\mathrm{l}}, \\
&\dot{\psi}_{\mathrm{r}}=\dot{\psi}_{\mathrm{l}},
\end{aligned} \quad (15)$$

where $\mathrm{d}_{\mathrm{x}}=\mathrm{l}_{\mathrm{lf}}^{\mathrm{d}} \cos \varphi_{\mathrm{lf}}^{\mathrm{d}}$, $\mathrm{d}_{\mathrm{y}}=\mathrm{l}_{\mathrm{lf}}^{\mathrm{d}} \sin \varphi_{\mathrm{lf}}^{\mathrm{d}}$, and $\overline{\mathrm{v}}_{\mathrm{l}}=\mathrm{v}_{\mathrm{l}}+\epsilon \mathrm{r}_{\mathrm{l}}$. The reference vehicle's dynamics (15) can be rewritten as

$$\begin{aligned}
&\dot{\mathrm{x}}_{\mathrm{r}}=\mathrm{u}_{\mathrm{r}} \cos \psi_{\mathrm{l}}-\mathrm{v}_{\mathrm{r}} \sin \psi_{\mathrm{l}}, \\
&\dot{\mathrm{y}}_{\mathrm{r}}=\mathrm{u}_{\mathrm{r}} \sin \psi_{\mathrm{l}}+\mathrm{v}_{\mathrm{r}} \cos \psi_{\mathrm{l}}, \\
&\dot{\psi}_{\mathrm{r}}=\mathrm{r}_{\mathrm{l}},
\end{aligned} \quad (16)$$

where $\mathrm{u}_{\mathrm{r}}=\mathrm{u}_{\mathrm{l}}-\mathrm{d}_{\mathrm{y}} \mathrm{r}_{\mathrm{l}}$ and $\mathrm{v}_{\mathrm{r}}=\mathrm{v}_{\mathrm{l}}+\mathrm{d}_{\mathrm{x}} \mathrm{r}_{\mathrm{l}}$.

Step 1: Define the errors in the body-fixed frame as

$$\begin{aligned}
&\mathrm{x}_{\mathrm{be}}=\mathrm{x}_{\mathrm{e}} \cos \psi_{\mathrm{f}}+\mathrm{y}_{\mathrm{e}} \sin \psi_{\mathrm{f}}, \\
&\mathrm{y}_{\mathrm{be}}=-\mathrm{x}_{\mathrm{e}} \sin \psi_{\mathrm{f}}+\mathrm{y}_{\mathrm{e}} \cos \psi_{\mathrm{f}}, \\
&\widetilde{\psi}=\psi_{\mathrm{a}}-\psi_{\mathrm{f}},
\end{aligned} \quad (17)$$

where $\mathrm{x}_{\mathrm{e}}=\mathrm{x}_{\mathrm{r}}-\overline{\mathrm{x}}_{\mathrm{f}}$, $\mathrm{y}_{\mathrm{e}}=\mathrm{y}_{\mathrm{r}}-\overline{\mathrm{y}}_{\mathrm{f}}$, $\psi_{\mathrm{e}}=\psi_{\mathrm{r}}-\psi_{\mathrm{f}}$, x_{be} and y_{be} are the x- and y-coordinates of the position error in the body-fixed frame, y_{be} $\widetilde{\psi}$ is the yaw angle error between the approach angle ψ_{a} and the yaw angle ψ_{f} of the follower, x_{e} and $\mathrm{y}_{\mathrm{e}}$are the position errors for the x- and y-axes and ψ_{e} is the yaw angle error. Here, the approach angle ψ_{a} is defined as follows [15]:

$$\psi_{\mathrm{a}}=\beta \tanh\left(\mathrm{D}^{2} / \gamma\right)+\psi_{\mathrm{l}}\left(1-\tanh\left(\mathrm{D}^{2} / \gamma\right)\right),$$

$$\beta=\tan^{-1}\left(\frac{y_e}{x_e}\right)=\psi_f+\tan^{-1}\left(\frac{y_{be}}{x_{be}}\right),$$
$$D=\sqrt{x_e^2+y_e^2}=\sqrt{x_{xe}^2+y_{be}^2}.$$

Using (16), we can obtain the following error dynamics in the body-fixed frame:

$$\begin{aligned}\dot{x}_{be}&=\dot{x}_e\cos\psi_f-x_e r_f\sin\psi_f+\dot{y}_e\sin\psi_f+y_e\dot{r}_f\cos\psi_f\\&=-u_f+y_{be}r_f+u_r\cos\psi_e-v_r\sin\psi_e\\\dot{y}_{be}&=-\dot{x}_e\sin\psi_f-x_e r_f\cos\psi_f+\dot{y}_e\cos\psi_f-y_e\dot{r}_f\sin\psi_f\\&=-v_f-x_{be}r_f+u_r\sin\psi_e+v_r\cos\psi_e\\\dot{\tilde{\psi}}&=\dot{\psi}_a-r_f.\end{aligned}\tag{18}$$

We select the virtual controls $\bar{u}_f$ and $\bar{r}_f$ of the follower's surge velocity u_f and the yaw velocity r_f as follows:

$$\begin{aligned}\bar{u}_f&=k_1x_{be}+y_{be}r_f+u_r\cos\psi_e-v_r\sin\psi_e,\\\bar{r}_f&=k_2\tilde{\psi}+\dot{\psi}_a,\end{aligned}\tag{19}$$

where

$$\dot{\psi}_a=\left(\frac{x_{be}\dot{y}_{be}-y_{be}\dot{x}_{be}}{D^2}+r_f-r_l\right)\tanh\left(\frac{D^2}{\gamma}\right)+r_l$$
$$+\frac{2}{\gamma}\left(\beta-\psi_l\right)\left(x_{be}\dot{x}_{be}+y_{be}\dot{y}_{be}\right)\operatorname{sech}^2\left(\frac{D^2}{\gamma}\right),$$

and k_1 and k_2 are the control gains to be chosen in the stability analysis.

Step 2: Define the error surface as

$$s_1=u_f-u_v,\ s_2=r_f-r_v,\tag{20}$$

where the filtered signals u_v and r_v are obtained by passing the virtual controls $\bar{u}_f$ and $\bar{r}_f$ through the first-order filter as follows:

$$k_1\dot{u}_v+u_v=\bar{u}_f,\quad u_v(0)=\bar{u}_f(0),$$
$$k_2\dot{r}_v+r_v=\bar{r}_f,\quad r_v(0)=\bar{r}_f(0).$$

Here, k_1 and k_2 are positive constants. The time derivatives of s_1 and s_2 are then obtained as follows:

$$\begin{aligned}\dot{s}_1&=\dot{u}_f-\dot{u}_v=\varphi_1+\frac{1}{m_{11}}\tau_u-\dot{u}_v,\\&=\widehat{\varphi}_1+\widetilde{W}_1^T\Theta_1+\xi_1+\frac{1}{m_{11}}\tau_u-\dot{u}_v,\end{aligned}\tag{21}$$

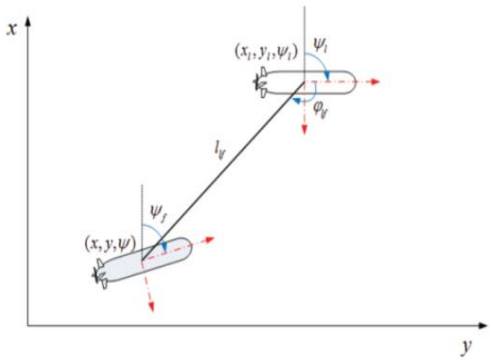

Figure 1. Leader-follower model of autonomous underwater vehicles.

$$\begin{aligned}\dot{s}_2&=\dot{r}_f-\dot{r}_v=\varphi_3+\frac{m_{22}}{m_{22}m_{33}-m_{23}^2}\tau_r-\dot{r}_v,\\&=\widehat{\varphi}_2+\widetilde{W}_2^T\Theta_2+\xi_2+\frac{m_{22}}{m_{22}m_{33}-m_{23}^2}\tau_r-\dot{r}_v.\end{aligned}\tag{22}$$

We choose the actual controls τ_u and τ_r as follows:

$$\begin{aligned}\tau_u&=m_{11}\left(-k_3s_1+\dot{u}_v+x_{be}-\left(\widehat{\varphi}_1+\widetilde{W}_1^T\Theta_1+\xi_1\right)\right),\\\tau_r&=\frac{m_{22}m_{33}-m_{23}^2}{m_{22}}\left(-k_4s_2+\dot{r}_v+\tilde{\psi}-\left(\widehat{\varphi}_2+\widetilde{W}_2^T\Theta_2+\xi_2\right)\right),\end{aligned}\tag{23}$$

where k_3 and k_4 are the control gains to be chosen in the stability analysis, $\widehat{\varphi}_1$ and $\widehat{\varphi}_2$ are, respectively, estimates of the unknown parameters φ_1 and φ_2, and are updated by

$$\dot{\widehat{W}}_1=\Gamma_1\Phi_1^Ts_1-\sigma_1\Gamma_1\widehat{W}_1,\tag{24}$$

$$\dot{\widehat{W}}_2=\Gamma_2\Phi_2^Ts_2-\sigma_2\Gamma_2\widehat{W}_2,\tag{25}$$

where Γ_1 and Γ_2 are positive definite matrices.

3.2 Stability Analysis

In this subsection, we show that all error signals of the closed-loop control system are uniformly ultimately bounded. Define the boundary layer errors as

$$\begin{aligned}e_1&=u_f-u_v,\\e_2&=v_f-v_v.\end{aligned}\tag{26}$$

Then, their time derivatives are

$$\begin{aligned}\dot{e}_1&=\dot{u}_v-\dot{\bar{u}}_f\\&=-\frac{e_1}{k_1}+\Xi_1\left(x_{be},y_{be},r_f,\psi_e,\dot{x}_{be},\dot{y}_{be},\dot{r}_f,\dot{\psi}_e\right),\\\dot{e}_2&=\dot{v}_v-\dot{\bar{v}}_f\\&=-\frac{e_2}{k_2}+\Xi_2\left(\psi_a,\psi_f,\dot{\psi}_a,\dot{\psi}_f,\ddot{\psi}_a\right).\end{aligned}\tag{27}$$

Theorem 1. Consider the underactuated AUV (1) with parametric uncertainties controlled by (23). If the proposed control system satisfies Assumption 1, and unknown parameters φ_1 and φ_2 are trained by the adaptation laws (24) and (25), respectively, then for V (0) μ, where μ is a positive constant, all error signals are uniformly ultimately bounded.

Proof. We choose the Lyapunov function as follows:

$$\begin{aligned} \mathrm{V}=\frac{1}{2}(&\mathrm{x}_{\mathrm{be}}^2+\widetilde{\psi}+\mathrm{s}_1^2+\mathrm{s}_2^2+\mathrm{e}_1^2+\mathrm{e}_2^2 \\ &+\widetilde{\mathrm{W}}_1^{\mathrm{T}}\Gamma_1^{-1}\widetilde{\mathrm{W}}_1+\widetilde{\mathrm{W}}_2^{\mathrm{T}}\Gamma_2^{-1}\widetilde{\mathrm{W}}_2), \end{aligned} \tag{28}$$

where Γ_1^{-1} and Γ_2^{-1} are positive definite matrices, and $\widetilde{\mathrm{W}}_{\mathrm{j}}$, j= 1, 2 are the estimation errors. The time derivative of (28) along with (18), (22), (26), and (27) yields

$$\begin{aligned} \dot{\mathrm{V}}=&\mathrm{x}_{\mathrm{be}}\left(-\mathrm{u}_{\mathrm{f}}+\mathrm{y}_{\mathrm{be}}\mathrm{r}_{\mathrm{f}}+\mathrm{u}_{\mathrm{r}}\cos\psi_{\mathrm{e}}-\mathrm{v}_{\mathrm{r}}\sin\psi_{\mathrm{e}}\right) \\ &+\widetilde{\psi}(\dot{\psi}_{\mathrm{a}}-\mathrm{r}_{\mathrm{f}})+\mathrm{s}_1\left(\widehat{\varphi}_1+\widetilde{\mathrm{W}}_1^{\mathrm{T}}\Theta_1+\xi_1+\frac{1}{\mathrm{m}_{11}}\tau_{\mathrm{u}}-\dot{\mathrm{u}}_{\mathrm{v}}\right) \\ &+\mathrm{s}_2\left(\widehat{\varphi}_2+\widetilde{\mathrm{W}}_2^{\mathrm{T}}\Theta_2+\xi_2+\frac{\mathrm{m}_{22}}{\mathrm{m}_{22}\mathrm{m}_{33}-\mathrm{m}_{23}^2}\tau_{\mathrm{r}}-\dot{\mathrm{r}}_{\mathrm{v}}\right) \\ &+\mathrm{e}_1\left(-\frac{\mathrm{e}_1}{\mathrm{k}_1}+\Xi_1\right)+\mathrm{e}_2\left(-\frac{\mathrm{e}_2}{\mathrm{k}_2}+\Xi_2\right) \\ &-\widetilde{\mathrm{W}}_1^{\mathrm{T}}\Gamma_1^{-1}\dot{\widehat{\mathrm{W}}}_1+\widetilde{\mathrm{W}}_2^{\mathrm{T}}\Gamma_2^{-1}\dot{\widehat{\mathrm{W}}}_2. \end{aligned} \tag{29}$$

Substituting (19), (23), (24), and (25) into (29) yields

$$\begin{aligned} \dot{\mathrm{V}}=&-\mathrm{k}_1\mathrm{x}_{\mathrm{be}}^2-\mathrm{k}_2\widetilde{\psi}^2-\mathrm{k}_3\mathrm{s}_1^2-\mathrm{k}_4\mathrm{s}_2^2-\frac{1}{\kappa_1}\mathrm{e}_1^2-\frac{1}{\kappa_2}\mathrm{e}_2^2 \\ &-\mathrm{e}_1\mathrm{x}_{\mathrm{be}}-\mathrm{e}_2\widetilde{\psi}+\mathrm{e}_1\Xi_1+\mathrm{e}_2\Xi_2 \\ &+\sigma_1\widetilde{\mathrm{W}}_1^{\mathrm{T}}\widehat{\mathrm{W}}_1+\sigma_2\widetilde{\mathrm{W}}_2^{\mathrm{T}}\widehat{\mathrm{W}}_2+\mathrm{s}_1\xi_1+\mathrm{s}_2\xi_2. \end{aligned} \tag{30}$$

From Assumption 1, (30) can be written as

$$\begin{aligned} \dot{\mathrm{V}}\le&-\mathrm{k}_1\mathrm{x}_{\mathrm{be}}^2-\mathrm{k}_2\widetilde{\psi}^2-\mathrm{k}_3\mathrm{s}_1^2-\mathrm{k}_4\mathrm{s}_2^2-\frac{1}{\kappa_1}\mathrm{e}_1^2 \\ &-\frac{1}{\kappa_2}\mathrm{e}_2^2+|\mathrm{e}_1|\,|\mathrm{x}_{\mathrm{be}}|+|\mathrm{e}_2|\left|\widetilde{\psi}\right|+\mathrm{e}_1\Xi_1+\mathrm{e}_2\Xi_2 \\ &+\mathrm{s}_1\xi_1+\mathrm{s}_2\xi_2-\frac{1}{2}\sigma_1\left\|\widetilde{\mathrm{W}}_1\right\|_{\mathrm{F}}^2-\frac{1}{2}\sigma_2\left\|\widetilde{\mathrm{W}}_2\right\|_{\mathrm{F}}^2 \\ &+\frac{1}{2}\sigma_1\mathrm{W}_{\mathrm{M},1}^2+\frac{1}{2}\sigma_2\mathrm{W}_{\mathrm{M},2}^2. \end{aligned} \tag{31}$$

Consider a set $\mathrm{A}:=\left[\mathrm{x}_{\mathrm{e}}^2+\widetilde{\psi}^2+\mathrm{s}_1^2+\mathrm{s}_2^2+\mathrm{e}_1^2+\mathrm{e}_2^2\le 2\mu\right]$. Since the set A is compact in $\mathbb{R}^7$, there exist positive constants p_{i} such that $|\Xi_{\mathrm{i}}|\le \mathrm{p}_{\mathrm{i}}$, i = 1, 2. Using Young's inequality, we have

$$\begin{aligned} \dot{\mathrm{V}}\le&-\left(\mathrm{k}_1-\frac{1}{2}\right)\mathrm{x}_{\mathrm{be}}^2-\left(\mathrm{k}_2-\frac{1}{2}\right)\widetilde{\psi}^2-\left(\mathrm{k}_3-\frac{1}{2}\right)\mathrm{s}_1^2 \\ &-(\mathrm{k}_4-\frac{1}{2})\mathrm{s}_2^2-(\frac{1}{\mathrm{k}_1}-\frac{1}{2})\mathrm{e}_1^2-(\frac{1}{\mathrm{k}_2}-\frac{1}{2})\mathrm{e}_2^2 \\ &-\frac{1}{2}\sigma_1\left\|\widetilde{\mathrm{W}}_1\right\|_{\mathrm{F}}^2-\frac{1}{2}\sigma_2\left\|\widetilde{\mathrm{W}}_2\right\|_{\mathrm{F}}^2-\left(1-\frac{\Xi_1^2}{\mathrm{p}_1^2}\right)\frac{\mathrm{p}_1^2\mathrm{e}_1^2}{2\epsilon_1} \\ &-\left(1-\frac{\Xi_2^2}{\mathrm{p}_2^2}\right)\frac{\mathrm{p}_2^2\mathrm{e}_2^2}{2\epsilon_2}+\frac{\epsilon_1}{2}+\frac{\epsilon_2}{2}+\frac{1}{2}\xi_1^2+\frac{1}{2}\xi_2^2, \end{aligned}$$

where ϵ_{i}, i = 1, 2, are positive constants. If we choose

$$\begin{aligned} &\mathrm{k}_1=\mathrm{k}_1^*+\frac{1}{2},\ \ \mathrm{k}_2=\mathrm{k}_2^*+\frac{1}{2},\ \ \mathrm{k}_3=\mathrm{k}_3^*+\frac{1}{2},\ \ \mathrm{k}_4=\mathrm{k}_4^*+\frac{1}{2}, \\ &\frac{1}{\kappa_1}=\kappa_1^*+\frac{\mathrm{p}_1^2}{2\epsilon_1}+1,\ \ \frac{1}{\kappa_2}=\kappa_2^*+\frac{\mathrm{p}_2^2}{2\epsilon_2}+1, \end{aligned}$$

where $\mathrm{k}_{\mathrm{i}}^*$ and κ_{i}^*, i = 1, 2, are positive constants, then we have

$$\begin{aligned} \dot{\mathrm{V}}\le&-\mathrm{k}_1^*\mathrm{x}_{\mathrm{be}}^2-\mathrm{k}_2^*\widetilde{\psi}_{\mathrm{e}}^2-\mathrm{k}_3^*\mathrm{s}_1^2-\mathrm{k}_4^*\mathrm{s}_2^2-\kappa_1^*\mathrm{e}_1^2-\kappa_2^*\mathrm{e}_2^2 \\ &-\frac{1}{2}\sigma_1\left\|\widetilde{\mathrm{W}}_1\right\|_{\mathrm{F}}^2-\frac{1}{2}\sigma_2\left\|\widetilde{\mathrm{W}}_2\right\|_{\mathrm{F}}^2+\delta_1 \\ \le&-\zeta_1\mathrm{V}+\delta_1, \end{aligned} \tag{32}$$

where $\delta_1=\frac{1}{2}\left(\epsilon_1+\epsilon_2+\xi_1^2+\xi_2^2+\sigma_1\mathrm{W}_{\mathrm{M},1}^2+\sigma_2\mathrm{W}_{\mathrm{M},2}^2\right)$.

The constant ζ_1 satisfies

$$0<\zeta_1<\min[\mathrm{k}_1^*,\ \mathrm{k}_2^*,\mathrm{k}_3^*,\mathrm{k}_4^*,\ \lambda_1^*,\lambda_2^*,\frac{1}{2}\sigma_1,\ \frac{1}{2}\sigma_2].$$

Multiplying (32) by $\mathrm{e}^{\zeta_1\mathrm{t}}$ yields

$$\frac{\mathrm{d}}{\mathrm{dt}}\left(\mathrm{V}\left(\mathrm{t}\right)\mathrm{e}^{\zeta_1\mathrm{t}}\right)\le\delta_1\mathrm{e}^{\zeta_1\mathrm{t}}. \tag{33}$$

Integrating (33) over [0, t] leads to

$$0\le\mathrm{V}\left(\mathrm{t}\right)\le\left[\mathrm{V}\left(0\right)-\frac{\delta_1}{\zeta_1}\right]\mathrm{e}^{-\zeta_1\mathrm{t}}+\frac{\delta_1}{\zeta_1}.$$

Since δ_1 is bounded, it follows that all error signals are uniformly ultimately bounded.

4. Simulation Results

In this section, we report the results of some computer simulations that illustrate the performance of the proposed formation controller for underactuated AUVs with parametric uncertainties. The surge force and the yaw moment of the leader of the

AUVs are chosen as follows:

$$0 \le \mathrm{t} \le 50, \quad \tau_{\mathrm{ul}} = 30, \quad \tau_{\mathrm{rl}} = 0,$$

$$50 < \mathrm{t} \le 100, \quad \tau_{\mathrm{ul}} = 30, \quad \tau_{\mathrm{rl}} = 3,$$

$$100 < \mathrm{t} \le 150, \quad \tau_{\mathrm{ul}} = 30, \quad \tau_{\mathrm{rl}} = -3,$$

$$150 < \mathrm{t} \le 200, \quad \tau_{\mathrm{ul}} = 30, \quad \tau_{\mathrm{rl}} = 0.$$

For the simulations, we select the initial conditions of the leader and the followers of the AUV as follows:

$$(\mathrm{x_l}(0), \mathrm{y_l}(0), \psi_{\mathrm{l}}(0)) = (0, 0, 0),$$

$$(\mathrm{x_{f1}}(0), \mathrm{y_{f1}}(0), \psi_{\mathrm{f1}}(0)) = (-1, 0, 0),$$

$$(\mathrm{x_{f2}}(0), \mathrm{y_{f2}}(0), \psi_{\mathrm{f2}}(0)) = (-1, 0, 0)$$

where the subscript l indicates a leader and the subscript $\mathrm{f_i}$, i = 1, 2, indicates followers: $\mathrm{x_l}$, $\mathrm{y_l}$, and ψ_{l} are the leader's positions on the x -axis, y-axis, and the leader's yaw angle, respectively. The desired formation parameters are as follows:

$$\mathrm{l^d_{lf1}} = 2;; \ \varphi^{\mathrm{d}}{}_{\mathrm{lf1}} = 3\pi/4,$$

$$\mathrm{l^d_{lf2}} = 2;; \ \varphi^{\mathrm{d}}{}_{\mathrm{lf2}} = -3\pi/4.$$

The control gains are chosen as $\mathrm{K_1}$ = 0.6, $\mathrm{K_2}$ = 1, $\mathrm{K_3}$ = 2, $\mathrm{K_4}$ = 3, $\mathrm{k_1}$=1, and $\mathrm{k_2}$ = 1. The parameters of the SRWNN are $\mathrm{N_i}$ = 3, $\mathrm{N_w}$ = 10, and $\Gamma_1 = \Gamma_2$ = diag[0.1], $\sigma_1 = \sigma_2 = 1$. The initial values of the weights are randomly given in the range of [-1, 1]. Various system parameters of a typical AUV for the simulations are given in Table 1.

Figure 2 shows the control result of formation control for the underactuated AUVs, where the trajectory of the leader (bold line) and the trajectories of the followers (dashed line and dash-dot line) are depicted. The proposed formation control algorithm requires the followers to maintain the desired distance and angle with respect to the leader. From the result of Figure 2, the followers move along the desired position with respect to the leader at the early stage of control. Figure 3 shows the actual surge velocity u, yaw velocity r, and control inputs, which are the yaw moment τ_{r} and surge force τ_{u}. The separation and bearing errors are shown in Figure 4. Each error stays in the neighborhood of zero at the early stage of control action.

Table 1. Parameters of the asymmetric AUV

Symbol	Parameter	Value	Unit
m	Mass	185	g
$\mathrm{I_z}$	Rotation inertia	50	$\mathrm{kgm^2}$
$\mathrm{X_{\dot{u}}}$	Added mass	-30	kg
$\mathrm{Y_{\dot{v}}}$	Added mass	-80	kg
$\mathrm{Y_{\dot{r}}}$	Added mass	-1	kg
$\mathrm{N_{\dot{r}}}$	Added mass	-30	$\mathrm{kgm^2}$
$\mathrm{Y_{rv}}$	Linear drag	0.1	kg
$\mathrm{Y_{vr}}$	Linear drag	0.1	kg
$\mathrm{N_{rv}}$	Linear drag	0.1	$\mathrm{kgm^2}$
$\mathrm{N_{vr}}$	Linear drag	0.1	$\mathrm{kgm^2}$
$\mathrm{N_v}$	Linear drag	0.01	$\mathrm{kgm^2}$
$\mathrm{N_{vv}}$	Linear drag	0.01	$\mathrm{kgm^2}$
$\mathrm{X_u}$	Surge linear drag	70	kg/s
$\mathrm{X_{u\|u\|}}$	Surge quadratic drag	100	kg/m
$\mathrm{Y_v}$	Sway linear drag	100	kg/s
$\mathrm{Y_{v\|v\|}}$	Sway quadratic drag	200	kg/m
$\mathrm{N_r}$	Yaw linear drag	50	$\mathrm{kgm^2/s}$
$\mathrm{N_{r\|r\|}}$	Quadratic yaw drag	100	$\mathrm{kgm^2}$
$\mathrm{x_g}$	Position of COG	0	m

AUV, autonomous underwater vehicle; COG, center of gravity.

5. Conclusion

We proposed a formation control algorithm for an underactuated AUV with parametric uncertainties. First, using the approach angle and formation error dynamics in the body-fixed frame, we solved the underactuated problem for AUVs. Second, the formation control algorithm was designed based on the leader-follower strategy. Third, the state transformation was used to deal with off-diagonal terms resulting from the differences in shapes between the bow and stern. Next, the parametric uncertainties of the AUV were estimated by a SRWNN. Finally, the formation control algorithm was designed based on the DSC method. From the simulation results, we confirmed that the proposed control algorithm can maintain the predefined formation with good performance.

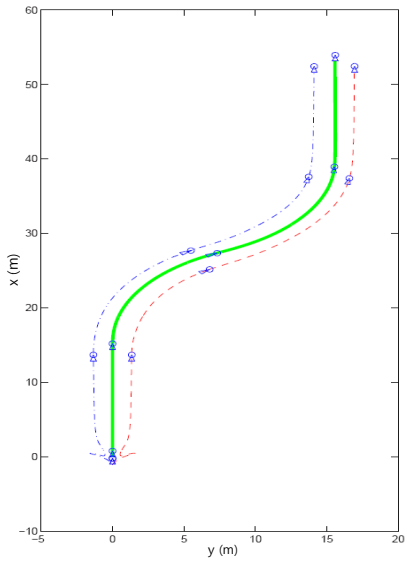

Figure 2. Control result for formation control (bold line, the trajectory of the leader; dashed line, the trajectory of the first follower; dash-dot line, the trajectory of the second follower).

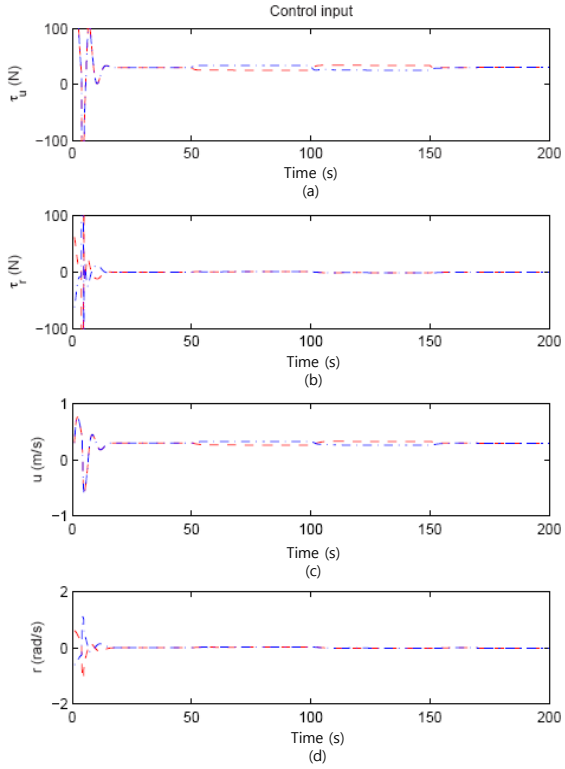

Figure 3. Control inputs for formation control: (a) surge force, (b) yaw moments, (c) surge velocities, (d) yaw velocities (dashed line, the control inputs of the first follower; dash-dot line, the control inputs of the second follower).

Conflict of Interest

No conflict of interest relevant to this article was reported.

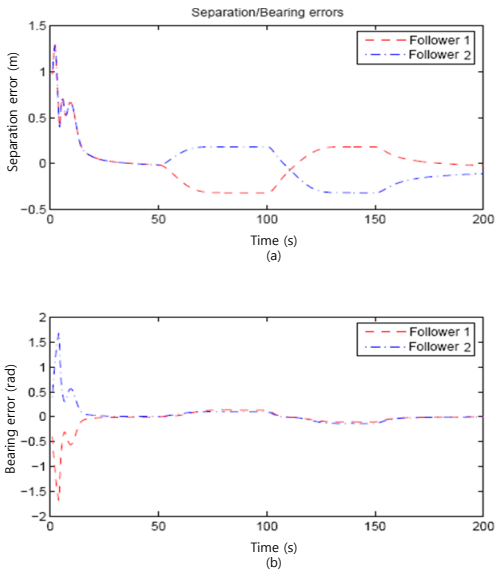

Figure 4. Formation errors: (a) separation errors, (b) bearing errors.

References

[1] F. A. Papoulias and Z. O. Oral, "Hopf bifurcation and nonlinear studies of gain margins in path control of marine vehicles," *Applied Ocean Research*, vol. 17, no. 1, pp. 21-32, Feb. 1995. http://dx.doi.org/10.1016/0141-1187(94)00016-G

[2] F. A. Papoulias, "Cross track error and proportional turning rate guidance of marine vehicles," *Journal of Ship Research*, vol. 38, no. 2, pp. 123-132, Jun. 1994.

[3] K. Y. Pettersen and H. Nijmeijer, "Underactuated ship tracking control: theory and experiments," *International Journal of Control*, vol. 74, no. 14, pp. 1435-1446, Jan. 2001. http://dx.doi.org/10.1080/00207170110072039

[4] E. Lefeber, K. Y. Pettersen, and H. Nijmeijer, "Tracking control of an underactuated ship," *IEEE Transactions on Control Systems Technology*, vol. 11, no. 1, pp. 52-61, Jan. 2003. http://dx.doi.org/10.1109/TCST.2002.806465

[5] Z. P. Jiang, "Global tracking control of underactuated ships by Lyapunov's direct method," *Automatica*, vol. 38, no. 1, pp. 301-309, Feb. 2002. http://dx.doi.org/10.1016/S0005-1098(01)00199-6

[6] T. Balch and R. C. Arkin, "Behavior-based formation control for multirobot teams," *IEEE Transactions on Robotics and Automation*, vol. 14, no. 6, pp. 926-939, Dec. 1998. http://dx.doi.org/10.1109/70.736776

[7] K. D. Do, "Practical formation control of multiple underactuated ships with limited sensing ranges," *Robotics and Autonomous Systems*, vol. 59, no. 6, pp. 457-471, Jun. 2011. http://dx.doi.org/10.1016/j.robot.2011.03.003

[8] M. A. Lewis and K. H. Tan, "High precision formation control of mobile robots using virtual structures," *Autonomous Robots*, vol. 4, no. 4, pp. 387-4-3, Oct. 1997. http://dx.doi.org/10.1023/A:1008814708459

[9] E. Yang and D. Gu, "Nonlinear formation-keeping and mooring control of multiple autonomous underwater vehicles," *IEEE Transactions on Mechatronics*, vol. 12, no. 2, pp. 164-178, Apr. 2007. http://dx.doi.org/10.1023/A:1008814708459

[10] R. Cui, S. S. Ge, B. V. E. How, and Y. S. Choo, "Leader follower formation control of underactuated autonomous underwater vehicles," *Ocean Engineering*, vol. 37, no. 17-18, pp. 1491-1502, Dec. 2010. http://dx.doi.org/10.1016/j.oceaneng.2010.07.006

[11] D. B. Edward, T. A. Beam, D. L. Odell, and M. L. Anderson, "A leader-follower algorithm for multiple AUV formations," in *Proceedings of IEEE/OES Autonomous Underwater Vehicles*, Sebasco, ME, Jun. 2004, pp.40-46. http://dx.doi.org/10.1109/AUV.2004.1431191

[12] R. Skjetne, S. Moi, and T. Fossen, "Nonlinear formation control of marine craft," in *Proceedings of the 41st IEEE Conference on Decision and Control*, Las Vegas, NV, Dec. 2002, pp. 1699-1704.

[13] K. D. Do, "Practical control of underactuated ships," *Ocean Engineering*, vol. 37, no. 13, pp. 1111-1119, Sep. 2010. http://dx.doi.org/10.1016/j.oceaneng.2010.04.007

[14] S. J. Yoo, Y. H. Choi, and J. B. Park, "Generalized predictive control based on self-recurrent wavelet neural network for stable path tracking of mobile robots: adaptive learning rate approach," *IEEE Transactions on Circuits and Systems I: Regular Papers*, vol. 53, no. 6, pp. 1381-1394, Jun. 2006. http://dx.doi.org/10.1109/TCSI.2006.875166

[15] B. S. Park, S. J. Yoo, J. B. Park, and Y. H. Choi, "A simple adaptive control approach for trajectory tracking of electrically driven nonholonomic mobile robots," *IEEE Transactions on Control Systems Technology*, vol. 18, no. 5, pp 1199-1206, Sep. 2010. http://dx.doi.org/10.1109/TCST.2009.2034639

[16] K. J. Kim, J. B. Park, and Y. H. Choi, "Path tracking control for underactuated autonomous underwater vehicles using approach angle," *IEICE Transactions on Fundamentals of Electronics, Communications and Computer Science*, vol. E95-A, no. 4, pp. 760-766, Apr. 2012. http://dx.doi.org/10.1587/transfun.E95.A.760

[17] D. Swaroop, J. K. Hedrick, P. P. Yip, and J. C. Gerdes, "Dynamic surface control for a class of nonlinear systems," *IEEE Transactions on Automatic Control*, vol. 45, no. 10, pp. 1893-1899, Oct. 2000. http://dx.doi.org/10.1109/TAC.2000.880994

[18] Y. Oussar, I. Rivals, L. Personnaz, and G. Dreyfus, "Training wavelet networks for nonlinear dynamic input-output modeling," *Neurocomputing*, vol. 20, no. 1-3, pp. 173-188, Aug. 1998. http://dx.doi.org/10.1016/S0925-2312(98)00010-1

[19] F. J. Lin, T. S. Lee, and C. H. Lin, "Robust H_∞ controller design with recurrent neural network for linear synchronous motor drive," *IEEE Transactions on Industrial Electronics*, vol. 50, no. 3, pp. 456-470, Jun. 2003. http://dx.doi.org/10.1109/TIE.2003.809394

[20] M. M. Polycarpou and M. J. Mears, "Stable adaptive tracking of uncertain systems using nonlinearly parameterized on-line approximators," *International Journal of Control*, vol. 70, no. 3, pp. 363-384, 1998. http://dx.doi.org/10.1080/002071798222280

Kyoung Joo Kim received the B.S. degree in Electrical Engineering from Yonsei University, Seoul,Korea, in 1998 and M.S. degree in Electrical and Electronic Engineering from Yonsei University, Seoul, Korea, in 2005. Currently, he is in the doctoral program in Electrical and Electronic Engineering from Yonsei University. His research interests include nonlinear control, autonomous underwater vehicle and path tracking control, etc.

Jin Bae Park received the B.S. degree in electrical Engineering from Yonsei University, Seoul, Korea, in l977 and M.S. and Ph.D. degrees in Electrical Engineering from Kansas State University, Manhattan, in 1985 and 1990, respectively. Since 1992, he has been with the Department of Electrical and Electronic Engineering, Yonsei University, Seoul, Korea, where he is currently a Professor. His

research interests include robust control and filtering. Nonlinear control, mobile robot, fuzzy logic control, neural networks, genetic algorithms and Hadamard-transform spectroscopy. He had served as vice-president for the Institute of Control, Automation, and Systems Engineers. He is serving as an Editor-in-chief for the International Journal of Control, Automation and Systems.

Yoon Ho Choi received the B.S.. M.S. and Ph.D. degree in Electrical Engineering from Yonsei University, Seoul, Korea, in 1980, 1982 and 1991, respectively. Since1993, he has been with Department of Electronic Engineering at Kyonggi University, where he is currently a Professor. From 2000 to 2002, he was with the Department of Electrical Engineering, Ohio State University, where he was a Visiting Scholar. His research interests include intelligent control, mobile robot, web-based control systems and wavelet transform. He was the Director for the Institute of Control. Automation and Systems Engineers from 2003 to 2004.